Ozonized 2-hydroxypropyl-β-cyclodextrins as novel materials with oxidative and bactericidal properties

Elsi Haddad, Marielle Pagès, Frédéric Violleau, Olivier Marsan, Marie-Hélène Manero, Romain Richard, Jean-Philippe Torré

Ozonized 2-hydroxypropyl-β-cyclodextrins as novel materials with oxidative and bactericidal properties

Elsi Haddad[a,c], Marielle Pagès[b,c], Frédéric Violleau[b,d], Olivier Marsan[e], Marie-Hélène Manero[a], Romain Richard[a], Jean-Philippe Torré[a,*]

[a] *Laboratoire de Génie Chimique, Université de Toulouse, CNRS, INPT, UPS, 4 Allée Emile Monso, 31432 Toulouse, France*

[b] *Plateforme TOAsT, Université de Toulouse, INP-PURPAN, 75 Voie du Toec, 31076 Toulouse, France*

[c] *Physiologie, Pathologie et Génétique Végétales (PPGV), Université de Toulouse, INP-PURPAN, 75 Voie du Toec, 31076 Toulouse, France*

[d] *Laboratoire de Chimie Agro-industrielle, LCA, Université de Toulouse, INRA, 4 Allée Emile Monso, 31000 Toulouse, France*

[e] *Centre Interuniversitaire de Recherche et d'Ingénierie des Matériaux, 4 Allée Emile Monso, 31432 Toulouse, France*

* Corresponding author: Jean-Philippe Torré. Email: *jean-philippe.torre@ensiacet.fr*

Abstract

Ozonized (2-Hydroxypropyl)-β-cyclodextrins (Oz-HPbCDs) were produced by direct gas/solid reaction between gaseous ozone (O_3) and solid HPbCD. The solid materials obtained were first characterized using physical and chemical methods and compared to the initial HPbCD. The main process parameters of the synthesis were studied independently to assess their effect on the oxidizing power of Oz-HPbCDs. The ability of the Oz-HPbCDs to retain their oxidative properties over time was evaluated, at different storage temperatures, for a period of at least two months. Lastly, aqueous solutions of HPbCD and Oz-HPbCD at different concentrations were contacted with bacterial strains of *Escherichia coli* and *Streptococcus uberis* to see whether these materials might have bactericidal properties. Since normal bacterial growth was noted with HPbCD, the antimicrobial efficiency of Oz-HPbCDs was clearly demonstrated on these two types of bacteria.

Keywords: Cyclodextrin; ozone; oxidant; material; antimicrobial activity; bactericide.

1. Introduction

Cyclodextrins (CDs) are cyclic oligosaccharides composed of bridged glucopyranose subunits, shaped like a truncated cone or a lampshade (see **Figures 1A** and **1B**) and forming a cavity at the center (Morin-Crini et al., 2021; Szejtli, 1998; Szejtli & Osa, 1996). CDs are used for their versatile inclusion properties in the food, pharmaceutical and biological industries among others (Harada, Takashima, &Yamaguchi, 2009; Li et al., 2014; McCray, Boving, & Brusseau, 2000). Despite the fact that these materials have been used and studied for decades (Szejtli, 1997; Szente, Szemán, & Sohajda, 2016), understanding the mechanisms at play is still a scientific challenge in many respects.

There are different types of CDs, the most common being composed of 6, 7 and 8 glucopyranose units, named α-CD, β-CD and γ-CD, respectively (Ibrahim & El-Zairy, 2009; Szejtli, 1998). These native CDs are obtained from the enzymatic degradation of starch under the action of the enzyme glucosyl-transferase (also called CGT-ase), meaning they have the same advantageous qualities as bio-based products. The hydrophobic nature of the cavity is due to the non-polar carbon skeleton. Conversely, the hydroxyl groups are what give the CD its hydrophilic exterior, meaning that these compounds are particularly soluble in aqueous media (Amiri & Amiri, 2017; Crini, 2014). The water solubility of β-CD can be greatly improved by modifying certain hydroxyl groups to break this hydrogen bond network. For example, the modified CD (2-hydroxypropyl)-β-cyclodextrin (HP-β-CD, written HPbCD for convenience in the following) is obtained industrially by treating the β-CD with propylene oxide in an alkaline medium (Nasongkla et al., 2003). This process makes it possible to substitute part of the hydroxyl functions for hydroxypropyl (HP) ones on the CD faces, as shown in **Figure 1**. HPbCDs can be characterized by their degree of substitution (*DS*), corresponding to the average number of HP functions present on the CD (the *DS* of HPbCDs usually ranges from 2.8 to 10.5), or their degree of molar substitution (*MS*), which gives the number of substituents per glucose unit (ranging from 0.4 to 1.5 for HPbCDs). HPbCDs have a high solubility in water (> 600 $g.L^{-1}$) (Loftsson & Duchêne, 2007), which is much greater than that of native β-CD (18.5 $g.L^{-1}$). As a high product solubility in water is advantageous for the biological applications targeted in this study, we therefore selected HPbCD as a relevant raw material for our experiments. Further information on the history, synthesis, properties and detailed characterizations of HPbCDs can be found in Malanga et al. (Malanga et al., 2016).

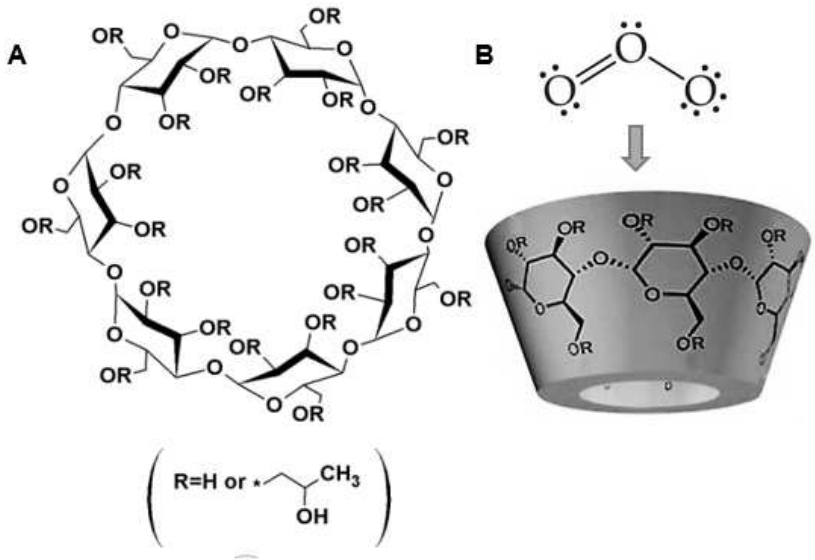

Figure 1. Example of the A) Molecular structure of (2-hydroxypropyl)-β-cyclodextrin, B) schematic view of the truncated cone-shape of the CD in contact with the ozone molecule.

The resistance of bacterial pathogens is increasing dramatically, resulting in multidrug resistance (MDR) to antibiotics. MDR bacteria are giving rise to serious health issues identified by several organizations such as the World Health Organization (WHO) and the European Centre for Disease Prevention and Control (ECDC). Studies are conducted by the European Food Safety Authority (EFSA) on the growing hazards of MDR bacteria in the food industry (Roca et al., 2015). The unreasonable use of antimicrobial agents has likewise caused this problem to spread to the natural environment (Wellington et al., 2013). This buildup should not be underestimated. The medical, food and agricultural sectors are faced with microbial issues, which can be dealt with by using chemicals such as pesticides. The French and European public authorities have introduced many regulations to control their use, but it appears necessary to propose more healthy and environmentally friendly alternatives (e.g. safer chemicals or less hazardous material) to better control microbial development.

Because of its oxidizing power and high effectiveness in killing bacteria, fungi, molds, and viruses (Cristiano, 2020), ozone is currently used for many applications such as wastewater treatment (Vittenet et al., 2015), air depollution (Vitola Pasetto et al., 2020) and is regarded as a very promising option for disinfection and sanitation measures (Tizaoui, 2020). Ozone is

also being looked at for potential applications such as crop protection, including treating plants and protecting fruit and vegetables like green peppers, raspberries and melons (Özen, Koyuncu, & Erbaş, 2021; Piechowiak, Grzelak-Błaszczyk, Sójka, & Balawejder, 2020; Zhang et al., 2021). In practice however, spraying ozone-enriched water on outdoor crops is a very difficult task due to the gas desorption phenomenon that occurs when the ozone-enriched water droplets come in contact with the air. The efficiency of this treatment is limited because ozone is so easily desorped from the water droplets (Canado et al., 2020). Moreover, ozone is well-known for its high instability due to its specificity of decomposing into oxygen very quickly (Muromachi, Ohmura, & Mori, 2012). Its half-life is about 20 minutes at ambient temperature when it is dissolved in water. Although this property is interesting as it confers to ozone a very low remanence (Pagès, Kleiber, Pierron, & Violleau, 2016), the gas' instability is a severe disadvantage as it makes storage and transportation difficult. Ozone must be produced continuously, as close as possible to the place where it is used. Ozone gas is generally produced by a high-voltage electrical discharge (3 - 20 kV) through an oxygen flow (O_2) or air in a continuous gas flow. Concentrations of up to 13 wt% of O_3 in the gas phase can be obtained by means of ozone generators designed specifically for medium industrial applications. Despite the fact that this type of ozone production system is very popular for stationary applications ─ such as water treatment ─ these electrical devices are relatively difficult to use in mobile applications, such as the in-field treatment of leaves, vegetables and fruit.

The contacting of ozone with CDs is scarcely documented in the literature. Just a few authors have proposed different concepts and protocols with CDs, the aim being to try and stabilize the ozone molecule ─ due to its very short half-life ─ in the CD cavity. Wang et al. (Wang, Peng, Li, Bai, & Huang, 2016) studied the complexation of HPbCD with O_3 in solution and observed its oxidative properties on potassium indigotrisulfonate (indigo) and 2.2'-azino-bis (3-ethylbenzothiazoline-6-sulfonate) (ABTS). They showed that only the solution containing HPbCD/O_3 decreased the indigo absorbance after 72 hrs. at 600 nm, and that the decomposition of ABTS increased by increasing the doses of ozone/CD solution. Dettmer et al. (Dettmer et al., 2017) concluded that O_3 can be stabilized with cyclodextrin in an aqueous solution and they showed that the half-life of O_3 increases proportionally with the HPbCD/O_3 molar ratio. The formation of an inclusion complex of O_3, trichloroethene (TCE), 1,1,1-trichloroethane (TCA) and 1,4-dioxane (1,4-D) with HPbCD was investigated by Khan et al. (Khan, Johnson, & Carroll, 2018) to remove the guest contaminants (TCE, TCA and 1,4-D) or

apply reagents during water treatment. Recently, Fan et al. (Fan et al., 2021) used nanobubble technology in an HPbCD inclusion to remove organic micropollutants from contaminated water. Nanobubbles increased the solubilization of O_3 and, according to the authors, formed an inclusion complex with HPbCD unlike macrobubbles. Using this technique, the removal proficiency of the main micropollutant 4-chlorophenol was found to be 6.9 higher compared to the standard macrobubble ozonation method. In all these studies, the CD-ozone contacting was always done in an aqueous solution with a prior step of CD solubilization in the water. Interestingly enough, to the best of the authors' knowledge, it is the first time that synthesis and characterization experiments with gaseous ozone contacting solid HPbCDs followed by tests of the ozonized CDs for biological applications, are presented.

The main target of this paper is therefore to report results on the synthesis and characterization of novel materials obtained by contacting gaseous ozone and solid cyclodextrins, and to evaluate their antimicrobial activity for potential biological applications. The key hypothesis suggests that CDs are oxidative materials, that physical and chemical changes are visible compared to native CDs, and that they have bactericidal properties. The results of physical and chemical characterizations of the HPbCD and ozonized HPbCD (denoted Oz-HPbCD) are discussed first. Then, the effect of the main process parameters on the oxidative power of the Oz-HPbCD obtained by direct gas/solid reaction are presented. The stability of the oxidative properties of the ozonized CDs stored at different temperatures for several months is also evaluated. Finally, to illustrate potential applications of these types of oxidative materials in microbiological treatments, the antimicrobial efficiency of ozonized CDs is studied.

2. Materials and methods

2.1. Materials

(2-Hydroxypropyl)-β-cyclodextrin (HPbCD) (purity ≥ 94%, *MS* = 0.9, produced by Wacker Chemie AG, Burghausen, Germany) was purchased from Sigma-Aldrich, and used without further purification. The chemicals used for the iodometric method were potassium iodide (KI) (reagent grade), sulfuric acid at 1 $mol.L^{-1}$ (purity ≥ 99.9%) purchased from Fisher Scientific, and a sodium thiosulfate solution at 1 $mol.L^{-1}$ provided by Merck. The potassium bromide (KBr) for IR spectroscopy Uvasol® (purity ≥ 99%) was purchased from Merck KBaA, Darmstadt, Germany. Ultra-pure water was used in all preparations with an ELGA Purelab Option-Q 7 model from VWS (for chemical characterizations and oxidative power determination) and with a Millipore Milli-Q Integral 15 water purification system from Merck (for microbiological tests). Oxygen (purity > 99.999%, purchased from Air Liquide, France) was used to produce ozone in the experimental rig.

2.2. Methods

2.2.1. Synthesis protocol

The ozonized CDs are synthesized using an experimental rig at bench scale. A diagram of the different elements of the experimental rig used in this study is shown in **Figure 2**, and detailed technical information is given in **Appendix A (section A1)**.

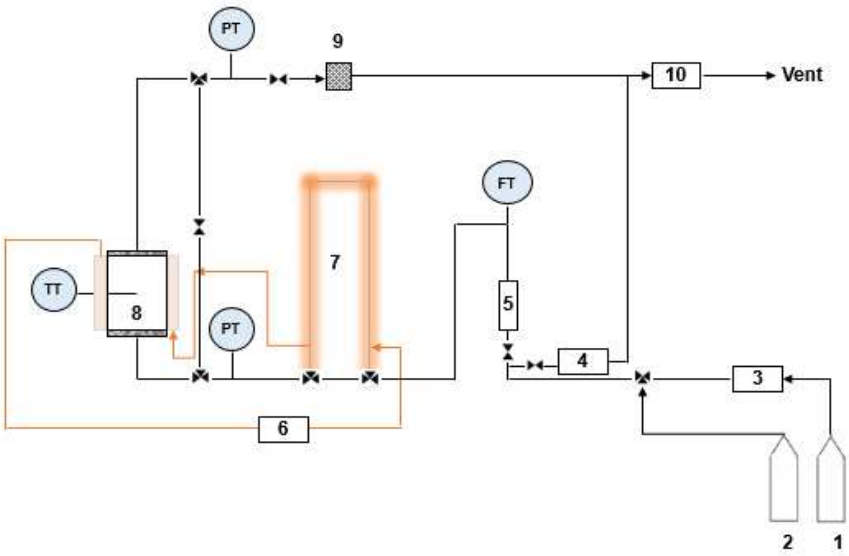

Figure 2. Process and instrumentation diagram of the experimental rig used for the synthesis:1. oxygen bottle; 2. nitrogen bottle; 3. ozonator; 4. ozone BMT analyzer; 5. float flowmeter; 6. thermostatic bath; 7. heat exchanger; 8. reactor; 9. filter; 10. ozone destructor; FT. mass flowmeter, TT. temperature probe; PT. pressure sensor

The reactor is first loaded with the HPbCD, directly on a balance with a precision of ± 0,005 g. A mass of ~ 5 g is used for the process parameter study and ~ 7 g are used for all the characterization studies. The reactor is then closed, the temperature probe connected to the supervision system, the reactor mounted on the rig, and the coolant hoses connected to the reactor jacket. Before starting the synthesis, a 5-minute leak test is always performed with nitrogen at 2 bar to ensure perfect sealing of all the pieces composing the rig. All the process lines are flushed with oxygen and the reactor, regulated at temperature (T_r), is first bypassed to start the ozone production. The pressure drop is adjusted in the by-pass line to equalize the pressure drop in the reactor to avoid any change in the gas flow when this line is closed. The gas flow (Q_f) and ozone concentration (C_{O3}) are then set to the correct values and stabilized using the reactor bypass line before the start of the synthesis. When all the process parameters are perfectly stable, the O_2/O_3 gas coming from the ozonator is sent to the reactor by turning the valves to shut the bypass line. The time $t = 0$ of the synthesis is defined at this moment. Contact between the ozone and the CD powder is then maintained for a given reaction time (noted t_r). At the end of the synthesis, the ozone concentration is gradually decreased to zero, and the ozonator is then switched off. After this, the reactor is vented with nitrogen, disassembled from the rig and transferred to a glove box (under air) to be opened safely. The ozonized CDs are finally discharged from the reactor into a capped glass vessel using a funnel. The product is immediately sampled for analysis and stored.

2.2.2. Oxidative power (*OP*)

The total oxidation capacity of the solid materials obtained from the synthesis is determined by iodometric titration carried out according to the following procedure: 20 mL of an aqueous solution of potassium iodide (KI) at 0.1 mol.L^{-1} is stirred in a 125-mL Erlenmeyer flask; then, the pH of the solution is adjusted to ~ 2 with few drops of sulfuric acid (1 mol.L^{-1}); finally, a precise amount of ozonized CD ($m_{oz\text{-}CD}$ ~ 0.05-0.1 g) measured at ± 10^{-4} g, is added to the acidified KI solution. The reactants are kept in contact under stirring for 60 minutes before titration.

The oxidative power of the material, noted *OP*, is therefore directly proportional to the quantity of iodine generated. The *OP,* expressed here as the ratio of the mass of iodine produced to the mass of *Oz-HPbCD*, is calculated by **Eq. (1)** as follows:

$$OP[\frac{mg_{I_2}}{g_{Oz-HPbCD}}] = \frac{C_{thio} \cdot \mathrm{V_{thio}} \cdot M_{I_2} \cdot 10^3}{2\, m_{Oz-HPbCD}} \quad (1)$$

with M_{I2} the molar mass of diiode (253.81 g.mol^{-1}), C_{thio} the concentration of the thiosulfate solution, V_{thio} the volume of the thiosulfate solution poured at equivalence, and $m_{Oz\text{-}HPbCD}$ the mass of ozonized CDs.

The decrease in the oxidative properties of the material during the storage time (t_s) is quantified by the rate at which oxidative power is lost (noted OP_{loss}). This indicator quantifies the stability of the *OP* versus time: the lower OP_{loss} , the more stable the oxidative properties of the product over time. OP_{loss} (in %) is defined as the difference in *OP* between the initial *OP* (measured at t_s = 0) and the *OP* measured at the storage time t_s, normalized by the initial *OP* obtained at t_s = 0. The OP_{loss} is expressed by **Eq. (2)** as follows:

$$OP_{loss}\ [\%] = \left(1 - \frac{OP_{ts}}{OP_{ts=0}}\right) \times 100$$

(2)

With $OP_{ts}=0$, *OP* at t_s = 0 and OP_{ts} the *OP* at t_s.

To ensure a robust determination of the *OP*, the iodometric titration is triplicated for each sample, and the given *OP* is the arithmetic mean of these 3 values.

2.2.3. Physico-chemical characterizations

224 The morphology of the particle before and after the synthesis is observed by scanning electron
225 microscopy (SEM), and the size distribution of the particles by granulometric analysis based
226 on light diffraction. Helium pycnometry is used to measure the real density (ρ) of the
227 particles, and the specific area ($a_{s,BET}$) of the samples is obtained from N_2 adsorption-
228 desorption isotherms at 77 K. The CDs before and after synthesis are characterized using FT-
229 IR and Raman vibrational spectroscopies. Details of the techniques and methods are given in
230 **Appendix A (section A2)**.
231
232 **2.2.4. Antimicrobial activity assessment**
233
234 ***Preculture of bacteria.*** The different bacterial strains (*Escherichia coli* L.1112 and
235 *Streptococcus uberis* L.1111) are stored in glycerol milk at −80°C. After thawing, 50 µL are
236 cultured in 5 mL of brain-heart broth (BHB) (Biokar diagnostics BK015HA). These
237 suspensions are incubated at 37°C under agitation (≈150 rpm) until bacterial growth is visible
238 (cloudy culture medium). On the day of the experiment, 100 µL of the bacterial preculture are
239 placed in 10 mL of BHB and incubated at 37°C under agitation at 150 rpm (in triplicate for
240 each strain). A tube of pure broth serves as a blank. The optical density at 600 nm (UV
241 Jenway ThermoFisher Scientific) is then measured for each suspension. The values obtained
242 are used to dilute bacterial suspensions in order to obtain bacterial inocula standardized at
243 5.10^5 CFU/mL.
244
245 ***Minimum Inhibitory Concentrations (MIC)*** are used to assess the antibacterial activity of the
246 ozonized powder and are determined by means of the microdilution method principle (CLSI,
247 2012). Solutions of Oz-HPbCD and HPbCD at seven different concentrations (between 30
248 and 0.003 $g.L^{-1}$) are prepared in brain-heart broth. The solutions are distributed over 48 wells
249 on 96-well microplates, as shown in **Appendix A (section A3, Figure A1)**. The highest
250 concentration of the powder (50 µL/well) is deposited in three wells in the first row (line 1).
251 Following the same configuration, decreasing concentrations are placed in wells from rows 2
252 to 7. 50 µL of bacterial suspension are added to the first two wells for each different dilution
253 (total volume 100 µL in each well) whereas 50 µL of BHB are added to the last well of each
254 row. The last row (no. 8) holds 50 µL of the bacterial suspension and 50 µL of the BHB
255 (positive control). The final concentration of the bacterial suspensions is therefore $2.5.10^5$
256 CFU/mL and those of the ozonized and non-ozonized HPbCD are between 15 and 0.0015 $g.L^-$

257 [1]. The microplates are placed in an incubator shaker (TECAN infinite M200 PRO) at 37°C
258 and 125 rpm for 24 hrs. After this period, the measured absorbance is 600 nm in each well.
259 This experiment is triplicated. Using this method, it is possible to simultaneously test the
260 effects of HPbCD and Oz-HPbCD on bacteria. Antimicrobial activity is assessed on two
261 bacterial strains: *Escherichia coli* and *Streptococcus uberis.* MICs are determined as the
262 minimum concentrations of HPbCD and/or Oz-HPbCD stopping the proliferation of bacteria.
263

264 # 3. Results and Discussion

265

266 ## 3.1 Physical and chemical characterization

267 In order to compare the particles before and after ozonation (i.e. HPbCD and Oz-HPbCD,
268 respectively), the results of the physical characterizations of the powders are presented first.
269 Concerning the morphology of the powders, the SEM images of both samples presented in
270 **Figures 3A** and **3B**, show spheroidal faceted particles of various sizes, presenting (in most
271 cases) a smooth surface perforated by numerous holes, with the smallest particles visible
272 inside the largest spheres. No salient differences can therefore be noted between the particles
273 before (**Figure 3C**) and after ozonation (**Figure 3D**).

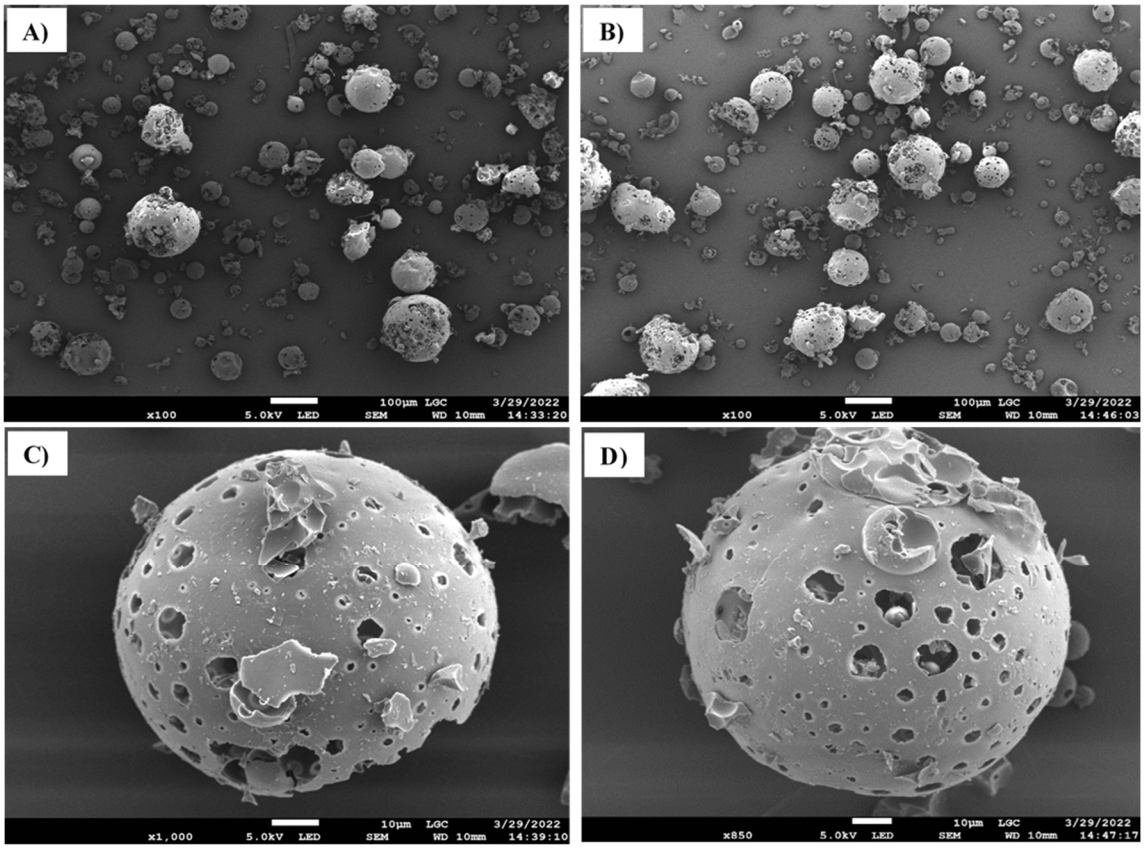

Figure 3. SEM images of the materials. A) and C) : HPbCD; B) and D): Oz-HPbCD; the scale (horizontal white bar at the bottom of the picture) is 100 µm for A) and B), and 10 µm for C) and D).

Table 1. Densities, specific surface areas, and median particle diameters of *HPbCD* and *Oz-HPbCD*

Physical characterization	ρ (g.cm^{-3})	$a_{s,BET}$ (m^2.g^{-1})	*Dv(50)* (µm)
HPbCD	1.3199 ± 0.0071	0.39 ± 0.01	42.3 ± 0.2
Oz-HPbCD	1.3062 ± 0.0073	0.43 ± 0.01	42.3 ± 0.2

The real particle densities (ρ), specific surface areas ($a_{s,BET}$) and median particle diameters (D_v50, i.e. the point in size distribution below which 50% of the material is contained) of the HPbCD and Oz-HPbCD, are presented in **Table 1**. Given the very small differences between the values and considering their absolute uncertainties, it can be concluded that ozonation has no effect on the physical parameters in these conditions. No variation in the specific surface area proves that the contact of HPbCD with ozone creates no meso/microporosity inside the particles. In addition, the fact that the D_v50 was exactly the same between the initial and final products demonstrates that the phenomena of fragmentation, attrition and dislocation of the initial particles during the synthesis are negligible in our case.

288 To characterize the possible chemical transformation after contact of the CD with O_3, HPbCD
289 and Oz-HPbCD were analyzed using FT-IR and Raman spectroscopy. Note that these two
290 techniques are complementary, particularly when the molecules are not symmetrical (Farber
291 et al., 2019). FT-IR and Raman spectra are shown in **Figure 4** and **Figure 5**, respectively.

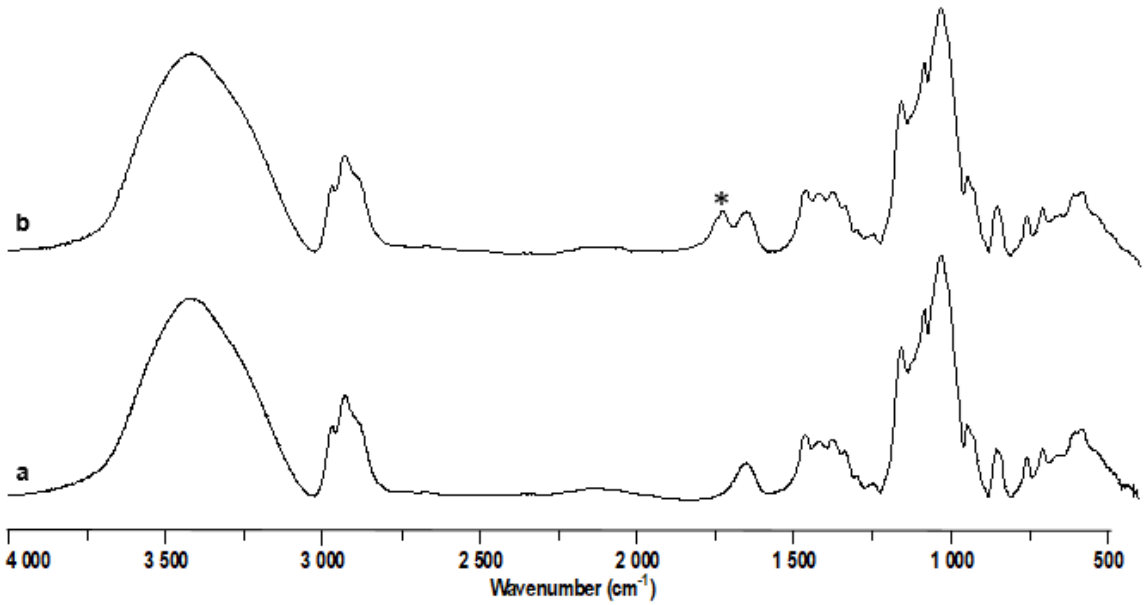

292

293 **Figure 4.** FTIR spectra of a) HPbCD, b) Oz-HPbCD . (*) new peak identified on the spectrum.

294

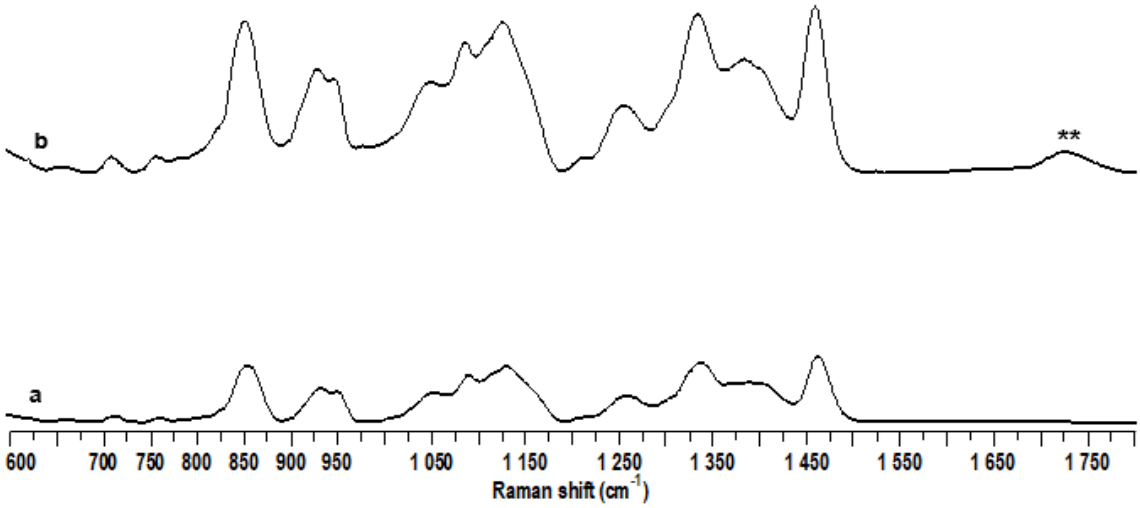

295

296 **Figure 5.** Raman spectra of a) HPbCD, b) Oz-HPbCD. (**) new peak identified on the spectrum.

297

298 As shown in **Figure 4**, both the HPbCD and Oz-HPbCD spectra reveal strong bands at 3,300
299 cm^{-1} (O─H stretching vibrations), 2,930 cm^{-1} (C─H stretching vibrations), 1,160 cm^{-1}, 1,090

300 cm^{-1} and 1,031 cm^{-1} corresponding to C─H, C─O stretching vibrations (Stancanelli et al.,
301 2008), and 1,650 cm^{-1} corresponding to O─H bending vibrations of the water molecules
302 physisorpbed or stabilized in the CDs (Yuan, Liu, & Liu, 2015). A new peak is clearly
303 noticeable at 1,730 cm^{-1} in the spectrum of Oz-HPbCD (identified by the * in **Figure 4**),
304 which could be attributed to the —C=O stretching of carbonyl groups.

305 The Raman spectra of HPbCD and Oz-HPbCD shown in **Figure 5** exhibit strong peaks at
306 1,460 cm^{-1} and 1,330 cm^{-1} corresponding to C─H bending and 1,135 cm^{-1}, 1,083 cm^{-1} and
307 1,048 cm^{-1} which can be correlated with C─O stretching (Egyed, 1990; Martins et al., 2017).
308 Again, a clear difference exists between the two spectra with the presence of a new peak at
309 1,728 cm^{-1} in the Oz-HPbCD spectrum (identified by the ** in **Figure 5**). This contribution
310 may be attributed to the creation of novel carbonyl groups by ozonation of the native CD, in
311 agreement with the FT-IR results.
312
313 It can therefore be inferred from these characterization results that, in these conditions, the
314 ozonation of HPbCD did not induce noticeable changes in the physical parameters considered
315 for this study, i.e. particle morphology, density, specific surface area and median particle
316 diameter. However, as new vibrational contributions were detected both by FT-IR and Raman
317 spectroscopy on the spectra of the ozonized CD, this means that chemical changes did occur
318 in the product during ozonation. And it seems logical that, in the presence of ozone, some of
319 the primary and secondary alcohols initially present in the HPbCD could be oxidized to form
320 different types of new organic functions such as aldehydes, ketones, carboxylic acids,
321 peracids and so on. These functions could either be linked (i.e. chemically attached) to the
322 CDs, or found in organic by-products if some parts of the CDs were broken by ozonation.
323 However, we are aware that a detailed quantitative analysis will be necessary, using NMR for
324 example, to identify and precisely determine the possible chemical modifications of the CDs
325 and any by-product(s) that may form in these conditions.
326

327 **3.2 Influence of the process parameters on *OP* values**

328 In order to provide robust information as regards the reproducibility of the experiments, 5
329 syntheses were carried out in the same process conditions. The mean average values of the
330 synthesis parameters were: Q_f = 49 Nl/h, C_{O3} = 96 g_{O3}/Nm^3, T_r = 25.8°C, and t_r = 2 hrs. The
331 measurement uncertainties of the process parameters Q_f, C_{O3}, and T_r, calculated as the average

of the standard deviations of each parameter obtained for the 5 experiments, were estimated to be ΔQ_f = ± 3 Nl/h, ΔC_{O3} = ± 3 g_{O3}/Nm^3, and ΔT_r = ± 0.8°C.

Based on all the experiments carried out, we noted that when the solid HPbCD was in contact with gaseous ozone, an exothermic phenomenon occurred inside the reactor, leading to an increase in temperature of about 5.0 ± 1.5°C. Immediately after t_0, the reactor temperature increased rapidly, reached a maximum, and then progressively decreased to stabilize close to the temperature set for the synthesis. In these conditions, the maximum peak temperature was reached in a few minutes, and this exothermicity could be measured for a few dozen minutes from t_0. At the end of each synthesis, the oxidative power of the ozonized CDs was measured by iodometry, and the mean value and standard deviation of *OP* were equal to 45 mg_{I2} /$g_{Oz\text{-}HPbCD}$ and σ= 3 mg_{I2} /$g_{Oz\text{-}HPbCD}$, respectively. These observations and results highlight that: (i) the contact between HPbCD and ozone leads to exothermic reaction(s); (ii) the synthesis process and the *OP* determination method, both evaluated using a set of 5 independent and identical runs, give good reproducible results, with a ± 7% variation of the *OP* values ; and (iii) as the *OP* > 0, it is clear that the process of contacting gaseous ozone with solid HPbCD generates materials with oxidative properties.

The effect of the process parameters (i.e. the gas flow rate Q_f, the ozone concentration in the gas C_{O3}, the reactor temperature T_r) on the *OP* of the Oz-HPbCD was first studied more precisely by maintaining the reaction time at t_r = 2 hrs.: when one parameter varied (i.e. ranging from 33 to 723 $NL.h^{-1}$ for Q_f, from 31 to 165 g_{O3}/Nm^3 for C_{O3}, and from 7 to 77°C for T_r), the others were maintained at constant values at Q_f = 186 $NL.h^{-1}$, C_{O3} = 76 $g_{o3}.Nm^3$, and T_r = 25.5°C. Then, to study the effect of the reaction time t_r, the same methodology was used, using a higher gas flow rate value (Q_f = 330 $NL.h^{-1}$). The results obtained are presented **Figure 6.**

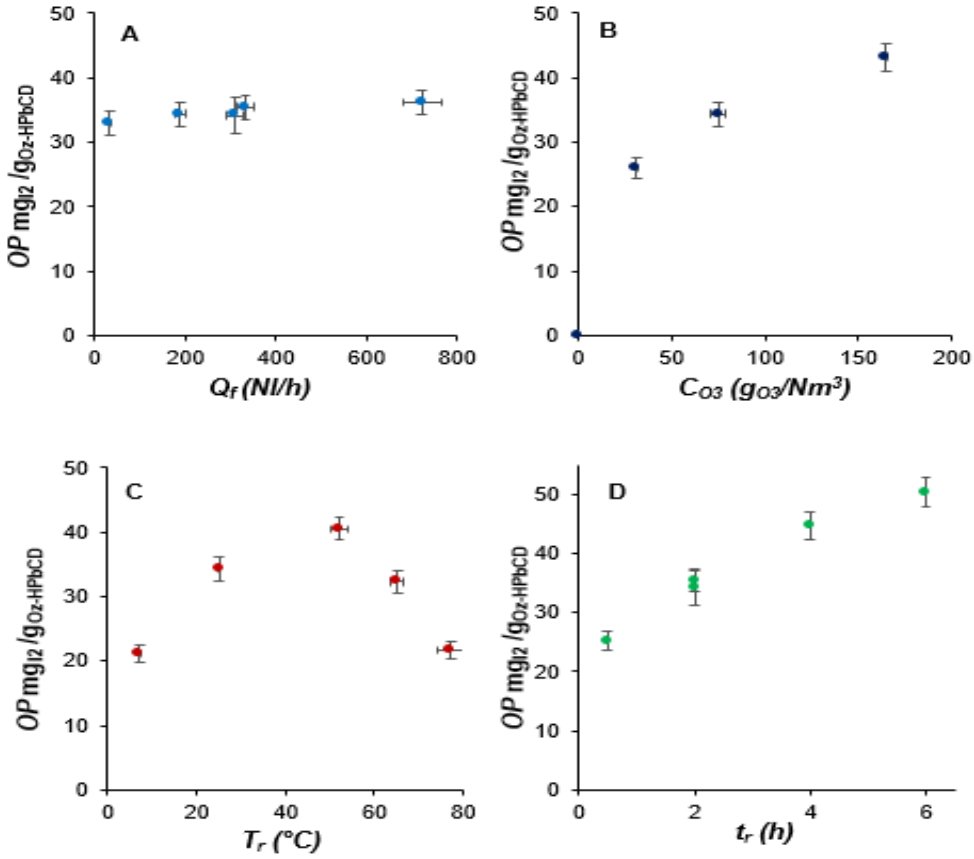

Figure 6. Effects of the different process parameters on the oxidative power of the Oz-HPbCD: A. gas flow rate; B. ozone concentration in the gas; C. mean reactor temperature; D. reaction time.

As shown in **Figure 6A,** the gas flow rate has a negligible effect on the *OP***,** as a variation in the *OP* of less than 10% (from 33 to 36 mg_{I2} /$g_{Oz\text{-}HPbCD}$) was measured across a very wide range of gas flow rates (from 33 to 723 Nl/h). As expected however, the *OP* was found to be strongly dependent of the ozone concentration in the gas as shown in **Figure 6B**: stepping up the C_{O3} from 31 to 165 g_{O3}/Nm^3 enhanced the *OP* of the Oz-HPbCD from 26 to 43 mg_{I2} /$g_{Oz\text{-}HPbCD}$. In an additional experiment performed using a gas containing only pure oxygen (C_{O3} = 0 g_{O3}/Nm^3), we found that the powder obtained at the end of the synthesis was not oxidant (the KI solution remained uncolored during the iodometric titration). As oxygen could also be a potential oxidizing agent, this latter point confirms with any doubt that the oxidative properties of the solid powder obtained at the end of the synthesis are due only to the presence of ozone in the O_2/O_3 gaseous mixture which contacts the CD. Interestingly enough, the mean reactor temperature had a singular non monotonic effect on the *OP* compared to the other parameters studied, as shown in **Figure 6C**: the *OP* variation curve first increases with T_r (*OP* = 21 to 40 mg_{I2} /$g_{Oz\text{-}HPbCD}$ when the temperature T_r goes from 7 to 52°C), reaches a maximum (extremum obviously located between ~ 30 and ~ 50°C), and finally drops from 40 to 21 mg_{I2}

/$g_{Oz\text{-}HPbCD}$ for temperatures between 52 and 77°C. Finally, it is clear from **Figure 6D** that increasing the reaction time of the synthesis significantly enhances the *OP* of the final ozonized product: the *OP* was increased from 25 to 50 mg_{I2} /$g_{Oz\text{-}HPbCD}$ when the reaction time was increased from 0,5 hrs. to 6 hrs., respectively.

As reaction kinetics are generally enhanced by a temperature increase, we initially expected that the *OP* would be higher at high synthesis temperatures. The fact that we obtained the exact opposite (i.e. we measured a drastic decrease in the *OP* for T_r > ~ 50°C) reveals a certain instability of the oxidative properties of the ozonized product at high temperature. This can be correlated with the creation of oxidative chemical functions on the ozonized CDs, and/or the encapsulation of oxidative species in the CD cavity, and/or the creation of by-products, which are unstable in these temperature conditions. For example, it is a well-known fact that the ozone molecule, as well as many peroxides (Batakliev, Georgiev, Anachkov, Rakovsky, & Zaikov, 2014), are naturally unstable from moderate to high temperatures. Because the oxidative power of the ozonized CD increased with the reaction time, with the ozone concentration in the gas and with the reactor temperature (for T_r < ~ 50°C) while being quasi-independent of the gas flow rate (i.e. the gas velocity inside the reactor), it is likely to be directly correlated with kinetics. The reaction and/or encapsulation did not appear to be limited by the external mass transfer (as the *OP* is independent of the velocity of the gas through the particles in the reactor), but it is likely it was limited by the reaction/encapsulation step and/or the diffusion of the gaseous ozone inside the solid CD particles. We therefore believe that it is possible that CDs did not react completely when in contact with ozone in these conditions. Unfortunately, it has been impossible to verify this assumption to date as the conversion (i.e. the fraction of the initial ozonized CDs) could not be determined in this study and requires additional specific characterizations with complementary analytical techniques, such as NMR. Work is in progress in this respect.

3.3. Stability study

In order to test the stability of the oxidizing power of the material over time, a synthesis was carried out in the following conditions: t_r = 6 hrs., Q_f = 335 Nl/hr., C_{O3} = 69 g_{O3}/Nm and T_r = 27.1°C. The stability test was performed using the same ozone treated with HPbCD. A mass of ~ 5 g of the powder obtained from the synthesis was separated into three equal parts (i.e. ~ 1.7 g), and each sample was stored in the same model of glass flask (sealed with a septum) under different temperatures: at ambient temperature at 21 ± 2°C, in a refrigerator at 2 ± 2°C,

411 and in a freezer at -19 ± 2°C. A sample was taken periodically in each flask to measure the
412 *OP* by iodometric titration. The analyses were performed over a period of 65 days. The loss of
413 the *OP* of the ozonized CD over time (t_s) for the three different storage temperatures is
414 presented in **Figure 7**.
415
416

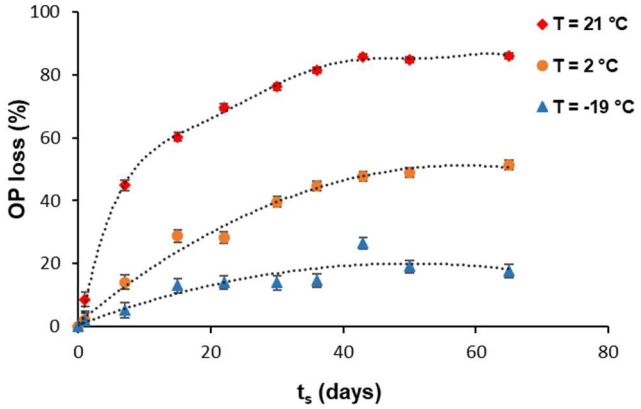

417
418 **Figure 7**. Evolution of the rate of the loss of OP (%) of the oxidative power over storage time (ts) for Oz-
419 HPbCD stored at different temperatures

420

421 After 65 days, the ozone-treated powder lost 86% of its *OP* when stored at 21°C, 51% at 2°C
422 and 18% at -19°C. Looking at these results, it is obvious that the stability of the ozonized CDs
423 depends strongly on the storage temperature of the materials: the lower the temperature, the
424 more stable the oxidative material. As the chemical characterization of the material revealed
425 that ozonation creates new chemical functions on the CDs and/or forms by-products, it might
426 be possible that the ozonized CDs contain oxidative products or functions, such as ozone, an
427 ozone derivative, or oxidative organic species such as peroxides. Such species might be
428 unstable during long storage periods under moderate or high temperatures (Clark, 2001). This
429 assumption is in agreement with the previous conclusions made in the section relative to the
430 effect of the process parameters, where it was shown that the *OP* significantly decreased when
431 the synthesis temperature was increased to values greater than 50°C. To improve our
432 understanding of the product stability over time, it might be interesting to perform additional
433 analytical experiments on the cyclodextrin samples, using NMR. Accordingly, it can be
434 concluded that these ozonized CDs are unstable in certain conditions, but are nevertheless
435 able to hold on to the most of their oxidative properties for a relatively long period of time

436 (more than two months) if the product is stored in a freezer at ~ -19 ± 2°C. In the light of
437 these results, we might expect to achieve an even better long-term stability over time if the
438 product is stored in hermetically closed vessels (instead of semi-hermetic flasks opened
439 regularly for sampling purposes).
440
441
442 **3.4. Minimum inhibitory concentrations (MIC)**
443
444 The results obtained for the MIC values are presented in **Figure 8** and **Figure 9** for the
445 bacterial strains *Streptococcus uberis* and *Escherichia coli* respectively. It is important to note
446 that these mean and standard deviation values result from 6 measurements, as each test
447 condition was replicated within the plate, and each plate was triplicated. The absorbance with
448 the different concentrations of powder for both strains was between 0.4 and 0.6. The positive
449 control, the bacterial suspension with the BHB, showed a normal bacterial growth. The well
450 with 15 $g.L^{-1}$ of the Oz-HPbCD solution exhibited 0 absorbance for both strains *Streptococcus*
451 *uberis* and *Escherichia coli*. However, at the same concentration, the wells with HPbCD
452 presented a normal growth. Antibacterial activity was therefore clearly visible with the
453 ozonized powder, although no difference was recorded between the two kinds of powder at
454 any of the lower concentrations (between 7.5 and 0.0015 $g.L^{-1}$). As no concentrations were
455 tested in the range between 7.5 and 15 $g.L^{-1}$, the MIC value for Oz-HPbCD is considered to
456 be 15 $g.L^{-1}$ and above.

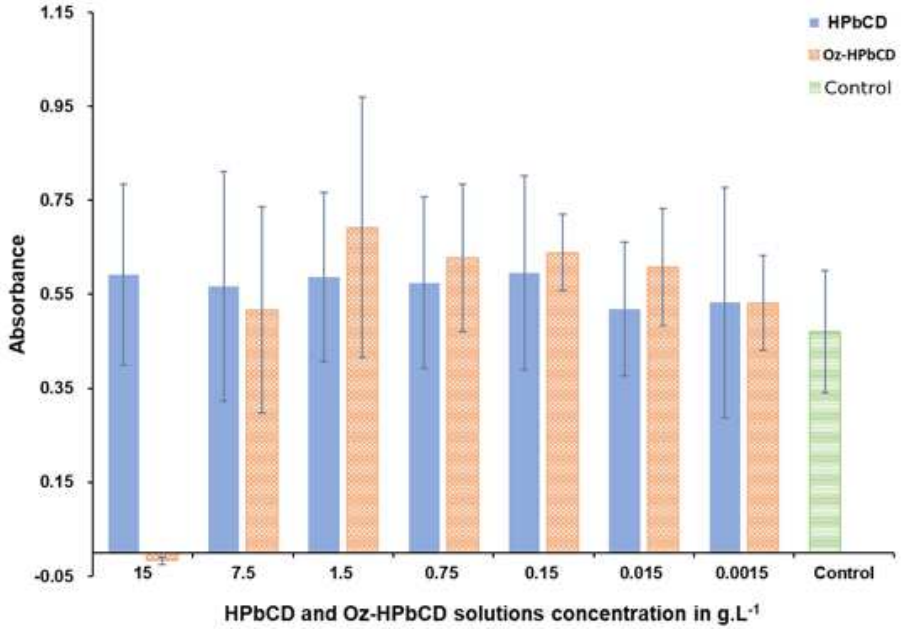

457

458 **Figure 8**. Antimicrobial activity assessment of HPbCD and Oz-HPbCD against the *Streptococcus uberis* strain.

459

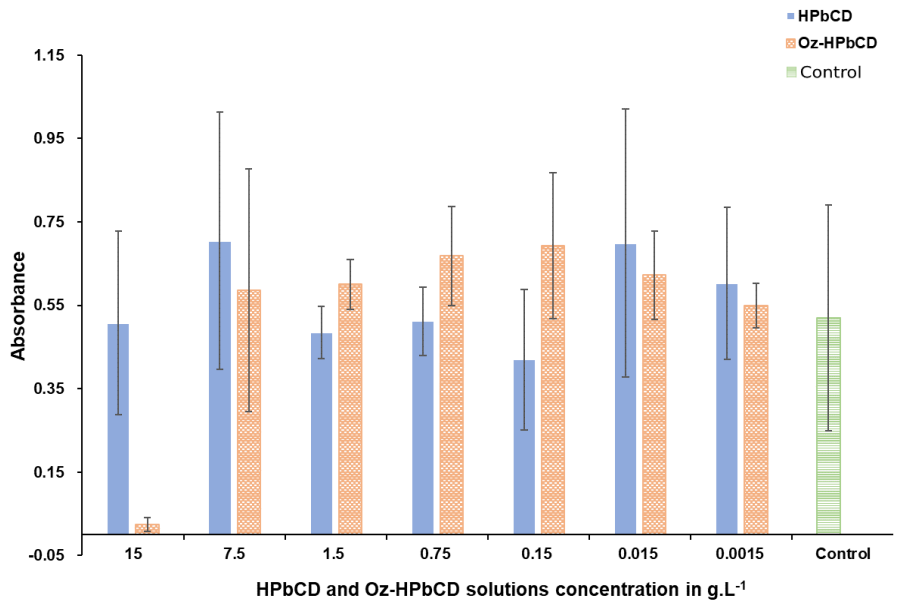

460

461 **Figure 9**. Antimicrobial activity assessment of HPbCD and Oz-HPbCD against the *Escherichia coli* strain.

462

463 # 4. Conclusion

464

The results obtained in this study demonstrate the possibility of producing solid oxidative materials by contacting gaseous ozone with HPbCD powder. Comparing the physical characterizations of the HPbCD used as raw material for the synthesis and that of the ozonized HPbCD, there was no apparent modification of the morphology of the solid particles, density, and specific area, leading to the conclusion that the contact with O_3 in these conditions does not induce fragmentation or the creation of meso/micro porosity in the initial particles. However, the characterization of Oz-HPbCD by FTIR and Raman spectroscopy revealed a new band which could be attributed to the –C=O stretching of carbonyl groups, demonstrating that the contact with O_3 leads to chemical modifications of the CDs, which may be directly related to new functions created on the CD and/or to the formation of by-products. Further analytical work, in particular NMR studies, will be required to more precisely identify and quantify both the by-products formed as a result of the synthesis and the chemical changes to the solid CDs by reaction with the ozone. Looking at the influence of the process parameters, the oxidative power (*OP*) of Oz-HPbCD was found to increase with the ozone concentration in the gas, the reactor temperature, and the duration of the synthesis, while the gas flow rate in the reactor had a low impact. These results seem to highlight the fact that the *OP* values are directly correlated with the reaction kinetics between CDs and O_3. The global reactivity is likely to be more limited by the chemical reactions and diffusivity of O_3 inside the solid particles than by the external mass transfer. It can therefore be hypothesized that, in the conditions of this study, the HPbCD particles may have not reacted completely. The Oz-HPbCDs, stored at low temperature were found to be relatively stable products, as only 18% of their oxidative properties were lost after 65 days in a freezer at -19°C. The microbiological results obtained by contacting Oz-HPbCDs and bacteria demonstrated that the ozonized products have bactericidal properties, with a minimum inhibitory concentration determined at $15 g.L^{-1}$ for both *Escherichia Coli* and *Streptococcus*. We believe that these results may open up new avenues for developing novel solid materials with tunable oxidative and antimicrobial properties, usable in biological applications.

Funding sources

This study benefited from funds provided by the French Region of Occitanie as part of the MOZART project, and from state aid managed by the National Research Agency under the

program Investments for the Future with the reference ANR-18-EURE-0021. This work was also supported by Toulouse Tech Transfer for potential valorization and technology transfer.

Author Contributions

The manuscript was written based on contributions from all the authors. All the authors have given their approval to the final version of the manuscript.

Declaration of competing interest

The authors declare that they have no known competing financial interests or personal relationships that could have appeared to influence the work reported in this paper.

Acknowledgements

We would like to acknowledge the French Region of Occitanie, the French National Research Agency (ANR), and Toulouse Tech Transfer (TTT) for their financial support of this work. We wish to thank the entire work group involved in the MOZART project, and more particularly Marie-Line de Solan Bethmale, Christine Rey-Rouch and Gwenaelle Guittier from the SAP for the analyses performed. We also extend our thanks to Kevin Dolin-Dolcy and Coralie Breton for their valuable help in the experiments. We would also like to acknowledge the technical staff of the LGC for their participation, particularly J.-L. Nadalin and Q. Ribière for prototyping and setting up instrumentation on the experimental rig.

References

Amiri, S., & Amiri, S. (2017). *Cyclodextrins: Properties and Industrial Applications* (1st ed). John Wiley & Sons Ltd, Hoboken, NJ, (Chapter 2). https://doi.org/10.1002/9781119247609.

Batakliev, T., Georgiev, V., Anachkov, M., Rakovsky, S., & Zaikov, G. E. (2014). Ozone decomposition. *Interdisciplinary toxicology*, *7*(2), 47–59. https://doi.org/10.2478/intox-2014-0008.

Canado, A., Tournois, M., Pages, M., Roustan, M., Remus-Borel, W., Dietrich, N., Violleau, F., & Hébrard, G. (2020). The sudden decrease of the dissolved ozone concentration in sprays: a mass transfer phenomenon? *Industrial & Engineering Chemistry Research*, *59*(33), 14914–14924. https://doi.org/10.1021/acs.iecr.0c03216.

Clark, D. E. (2001). Peroxides and peroxide-forming compounds. *Chemical Health & Safety*, *8*(5), 12–22. https://doi.org/10.1016/S1074-9098(01)00247-7.

CLSI (2012). *Methods for Dilution Antimicrobial Susceptibility Tests for Bacteria That Grow Aerobically*; Approved Standard—Ninth Edition. CLSI document M07-A9. Wayne, PA: Clinical and Laboratory Standards Institute.

Crini, G. (2014). Review: a history of cyclodextrins. *Chemical Reviews*, *114*(21), 10940-10975. https://doi.org/10.1021/cr500081p.

Cristiano, L. (2020). Could ozone be an effective disinfection measure against the novel coronavirus (SARS-CoV-2)? *Journal of Preventive Medicine and Hygiene*, *61*(3), E301-E303. https://doi.org/10.15167/2421-4248/jpmh2020.61.3.1596.

Dettmer, A., Ball, R., Boving, T.B., Khan, N.A., Schaub, T., Sudasinghe, N., Fernandez, C.A. & Carroll, K.C. (2017). Stabilization and prolonged reactivity of aqueous-phase ozone with cyclodextrin. *Journal of Contaminant Hydrology*, *196,* 1-9, https://doi.org/10.1016/j.jconhyd.2016.11.003.

Egyed, O. (1990). Spectroscopic studies on β-cyclodextrin. *Vibrational Spectroscopy*, *1*(2), 225-227. https://doi.org/10.1016/0924-2031(90)80041-2.

Fan, W., An, W., Huo, M., Xiao, D., Lyu, T. & Cui, J. (2021). An integrated approach using ozone nanobubble and cyclodextrin inclusion complexation to enhance the removal of micropollutants. *Water Research*, *196*, 117039. https://doi.org/10.1016/j.watres.2021.117039.

Farber, C., Li, J., Hager, E., Chemelewski, R., Mullet, J., Rogachev, Yu. A., & Kurouski, D. (2019). Complementarity of Raman and Infrared spectroscopy for structural characterization of plant epicuticular waxes. *ACS Omega*, *4*(2), 3700-3707. https://doi.org/10.1021/acsomega.8b03675.

Harada, A., Takashima, Y., & Yamaguchi, H. (2009). Cyclodextrin-based supramolecular polymers. *Chemical Society Reviews, 38, 875-885*. https://doi.org/10.1039/b705458k.

Ibrahim, N.A., & El-Zairy, E.M.R. (2009). Union disperse printing and UV-protecting of wool/polyester blend using a reactive β-cyclodextrin, *Carbohydrate Polymers, 76*(2), 244-249. https://doi.org/10.1016/j.carbpol.2008.10.020.

Khan, N. A., Johnson, M.D., & Carroll, K.C. (2018). Spectroscopic methods for aqueous cyclodextrin inclusion complex binding measurement for 1,4-dioxane, chlorinated co-contaminants, and ozone. *Journal of Contaminant Hydrology*, *210*, 31-41. https://doi.org/10.1016/j.jconhyd.2018.02.002.

Li, N., Chen, Y., Zhang, Y.M., Yang, Y., Su, Y., Chen, J.-T., & Liu, Y. (2014). Polysaccharide-gold nanocluster supramolecular conjugates as a versatile platform for the targeted delivery of anticancer drugs. *Scientific Reports*, *4*, 4164. https://doi.org/10.1038/srep04164.

Loftsson, T., & Duchêne, D. (2007). Cyclodextrins and their pharmaceutical applications. *International Journal of Pharmaceutics*, *329*(1–2), 1-11. https://doi.org/10.1016/j.ijpharm.2006.10.044.

Malanga, M., Szemán, J., Fenyvesi, E., Puskás, E., Csabai, K., Gyémánt, G., Fenyvesi, F., & Szente, L. (2016). "Back to the future": a new look at hydroxypropyl beta-cyclodextrins. *Journal of Pharmaceutical Sciences*, *105*(9), 2921-2931. https://doi.org/10.1016/j.xphs.2016.04.034.

Martins, M.L., Eckert, J., Jacobsen, H., Dos Santos, E.C., Ignazzi, R., Ribeiro de Araujo, D., Bellissent-Funel, M.-C., Natali, F., Marek Koza, M., Matic, A., De Paula, E., & Bordallo, H.N. (2017). Raman and Infrared spectroscopies and X-ray diffraction data on bupivacaine and ropivacaine complexed with 2-hydroxypropyl−β−cyclodextrin. Data in Brief, 15, 25-29. https://doi.org/10.1016/j.dib.2017.08.053.

McCray,J., Boving, T., & Brusseau, M. (2000). Cyclodextrin-enhanced solubilization of organic contaminants with implications for aquifer remediation. *Ground Water Monitoring & Remediation, 20*, 94-103. https://doi.org/10.1111/j.1745-6592.2000.tb00256.x.

Morin-Crini, N., Fourmentin, S., Fenyvesi, É., Lichtfouse, E., Torri, G., Fourmentin, M., & Crini, G. (2021). 130 years of cyclodextrin discovery for health, food, agriculture, and the industry: a review. *Environmental Chemistry Letters, 19*, 2581–2617. https://doi.org/10.1007/s10311-020-01156-w.

Muromachi, S., Ohmura, R., & Mori, Y. H. (2012). Phase equilibrium for ozone-containing hydrates formed from an (ozone + oxygen) gas mixture coexisting with gaseous carbon dioxide and liquid water. *The Journal of Chemical Thermodynamics*, *49*, 1-6. https://doi.org/10.1016/j.jct.2012.01.009.

Nasongkla, N., Wiedmann, A. F., Bruening, A., Beman, M., Ray, D., Bornmann, W. G., Boothman, D. A., & Gao, J. (2003). Enhancement of solubility and bioavailability of β-lapachone using cyclodextrin inclusion complexes. *Pharmaceutical Research*, *20*, 1626-1636. https://doi.org/10.1023/a:1026143519395.

Özen, T., Koyuncu, M.A. & Erbaş, D. (2021). Effect of ozone treatments on the removal of pesticide residues and postharvest quality in green pepper. Journal of Food Science and Technology, 58, 2186–2196, https://doi.org/10.1007/s13197-020-04729-3.

Pagès, M., Kleiber, D., Pierron, R. J. G., & Violleau, F. (2016). Ozone effects on *Botrytis cinerea* Conidia using a bubble column: germination inactivation and membrane phospholipids oxidation. *Ozone: Science & Engineering*, *38*(1), 62-69. https://doi.org/10.1080/01919512.2015.1074856.

Piechowiak, T., Grzelak-Błaszczyk, K., Sójka, M., & Balawejder, M. (2020). Changes in phenolic compounds profile and glutathione status in raspberry fruit during storage in ozone-enriched atmosphere. Postharvest Biology and Technology, 168, 111277. https://doi.org/10.1016/j.postharvbio.2020.111277.

Roca, I., Akova, M., Baquero, F., Carlet, J., Cavaleri, M., Coenen, S., Cohen, J., Findlay, D., Gyssens, I., Heure, O.E., Kahlmeter, G., Kruse, H., Laxminarayan, R., Liébana, E., López-Cerero, L., MacGowan, A., Martins, M., Rodríguez-Baño, J., Rolain, J.-M., Segovia, C., Sigauque, B., Tacconelli, E., Wellington, E., & Vila, J. (2015). The global threat of

antimicrobial resistance: science for intervention. *New Microbes and New Infections*, *6*, 22-29. https://doi.org/10.1016/j.nmni.2015.02.007.

Stancanelli, R., Ficarra, R. , Cannavà, C., Guardo, M., Calabrò, M.L., Ficarra, P., Ottanà, R., Maccari, R., Crupi, V., Majolino, D., & Venuti, V. (2008). UV–vis and FTIR-ATR characterization of 9-fluorenon-2-carboxyester/(2-hydroxypropyl)-β-cyclodextrin inclusion complex. *Journal of Pharmaceutical and Biomedical Analysis*, *47*(4-5), 704-709. https://doi.org/10.1016/j.jpba.2008.02.018.

Szejtli, J. (1998). Introduction and general overview of cyclodextrin chemistry. *Chemical Reviews*, *98*(5), 1743-1754. https://doi.org/10.1021/cr970022c.

Szejtli, J. (1997). Utilization of cyclodextrins in industrial products and processes. *Journal of Materials Chemistry, 7*(4), 575-585. https://doi.org/10.1039/A605235E.

Szejtli, J., & Osa, T. (1996). Comprehensive Supramolecular Chemistry, Volume 3: Cyclodextrins. (1st ed.). Oxford: Pergamon.

Szente, L., Szemán, J., Sohajda, T. (2016). Analytical characterization of cyclodextrins: History, official methods and recommended new techniques. *Journal of Pharmaceutical and Biomedical Analysis*, *130*, 347-365. https://doi.org/10.1016/j.jpba.2016.05.009.

Tizaoui, C. (2020). Ozone: a potential oxidant for COVID-19 Virus (SARS-CoV-2). *Ozone: Science & Engineering*, *42*(5), 378-385. https://doi.org/10.1080/01919512.2020.1795614.

Vitola Pasetto, L., Simon, V., Richard, R., Pic, J.-S., Violleau, F., & Manero, M.-H. (2020). A catalyst-free process for gas ozonation of reduced sulfur compounds. *Chemical Engineering Journal*, *387,* 123416. https://doi.org/10.1016/j.cej.2019.123416.

Vittenet, J., Aboussaoud, W., Mendret, J., Pic, J-S., Debellefontaine, H., Lesage, N., Faucher, K., Manero, M-H., Thibault-Starzyk, F., Leclerc, H., Galarneau, A., & Brosillon, S. (2015). Catalytic ozonation with γ-Al2O3 to enhance the degradation of refractory organics in water. *Applied Catalysis A: General*, *504*, 519–532. https://doi.org/10.1016/j.apcata.2014.10.037.

Wang, T., Peng, D., Li, Y., Bai, Y. & Huang, T. (2016). HP-β-Cyclodextrin assisted ozonation. *Proceedings of the 2016 International Conference on Civil, Transportation and Environment*, 1362-1365. Aug 28, 2016 - Aug 29, 2016, Phuket, Thailand. https://doi.org/10.2991/iccte-16.2016.239.

Wellington, E. M. H., Boxall, A. B. A., Cross, P., Feil, E. J., Gaze, W. H., Hawkey, P. M., Johnson-Rollings, A. S., Jones, D. L., Lee, N. M., Otten, W., Thomas, C. M., & Williams, A. P. (2013). The role of the natural environment in the emergence of antibiotic resistance in Gram-negative bacteria. *The Lancet Infectious Diseases, 13*(2), 155-165. https://doi.org/10.1016/S1473-3099(12)70317-1.

Yuan, C., Liu, B., & Liu, H. (2015). Characterization of hydroxypropyl-β-cyclodextrins with different substitution patterns via FTIR, GC–MS, and TG–DTA. *Carbohydrate Polymers*, *118*, 36-40. https://doi.org/10.1016/j.carbpol.2014.10.070.

Zhang, X., Tang, N., Zhang, H., Chen, C., Li, L., Dong, C., & Cheng, Y. (2021). Comparative transcriptomic analysis of cantaloupe melon under cold storage with ozone treatment. *Food Research International*, *140*, 109993. https://doi.org/10.1016/j.foodres.2020.109993.

GRAPHICAL ABSTRACT